



Calhoun: The NPS Institutional Archive

Theses and Dissertations

Thesis Collection

2007-09

Lagrangian observations of rip currents

Morrison, Jonathan David.

Monterey, California. Naval Postgraduate School

<http://hdl.handle.net/10945/3240>



Calhoun is a project of the Dudley Knox Library at NPS, furthering the precepts and goals of open government and government transparency. All information contained herein has been approved for release by the NPS Public Affairs Officer.

Dudley Knox Library / Naval Postgraduate School
411 Dyer Road / 1 University Circle
Monterey, California USA 93943

<http://www.nps.edu/library>



NAVAL POSTGRADUATE SCHOOL

MONTEREY, CALIFORNIA

THESIS

LAGRANGIAN OBSERVATIONS OF RIP CURRENTS

by

Jonathan David Morrison

September 2007

Thesis Advisor:
Second Reader:

Jamie MacMahan
Timothy Stanton

Approved for public release; distribution is unlimited

THIS PAGE INTENTIONALLY LEFT BLANK

REPORT DOCUMENTATION PAGE			<i>Form Approved OMB No. 0704-0188</i>	
Public reporting burden for this collection of information is estimated to average 1 hour per response, including the time for reviewing instruction, searching existing data sources, gathering and maintaining the data needed, and completing and reviewing the collection of information. Send comments regarding this burden estimate or any other aspect of this collection of information, including suggestions for reducing this burden, to Washington headquarters Services, Directorate for Information Operations and Reports, 1215 Jefferson Davis Highway, Suite 1204, Arlington, VA 22202-4302, and to the Office of Management and Budget, Paperwork Reduction Project (0704-0188) Washington DC 20503.				
1. AGENCY USE ONLY (Leave blank)		2. REPORT DATE September 2007	3. REPORT TYPE AND DATES COVERED Master's Thesis	
4. TITLE AND SUBTITLE Lagrangian Observations of Rip Currents			5. FUNDING NUMBERS	
6. AUTHOR(S) Jonathan David Morrison				
7. PERFORMING ORGANIZATION NAME(S) AND ADDRESS(ES) Naval Postgraduate School Monterey, CA 93943-5000			8. PERFORMING ORGANIZATION REPORT NUMBER	
9. SPONSORING /MONITORING AGENCY NAME(S) AND ADDRESS(ES) N/A			10. SPONSORING/MONITORING AGENCY REPORT NUMBER	
11. SUPPLEMENTARY NOTES The views expressed in this thesis are those of the author and do not reflect the official policy or position of the Department of Defense or the U.S. Government.				
12a. DISTRIBUTION / AVAILABILITY STATEMENT Approved for public release; distribution is unlimited.			12b. DISTRIBUTION CODE	
13. ABSTRACT (maximum 200 words) <p>A comprehensive field rip-current experiment (RCEX) was conducted from 14 April to 18 May 2007 in Sand City, California, on Monterey Bay. Lagrangian observations were made with inexpensive (\$150), handheld, Differential Global Positioning Systems (DGPS) mounted on surf zone drifters. The inexpensive DGPS requires post-processing to achieve $O(0.4m)$ position accuracy and $O(0.01m/s)$ velocity accuracy. Thirty drifters were constructed and deployed in well-developed, rip-currents to map the circulation patterns for the first time in the field at a high spatial resolution. Drifter observations obtained during three-hour periods on seven different days under varying wave and tidal conditions describe eddies with a rotational period of $4.7min$, confined to the surf-zone and coupled to the rip morphology. On average, three drifters per hour exited the surf-zone. Dependent upon wave conditions, one or two eddies existed between $90m$-spaced rip-channels, creating a seaward flow in the channels and shoreward flow over the shoals. Cross-shore volumetric flow rates for an alongshore transect through the eddy centers balance to a difference of less than 10% of the gross flow discharge. Velocity measurements obtained from drifter data are evaluated with velocities obtained from stationary, in-situ instruments.</p>				
14. SUBJECT TERMS Rip currents, Lagrangian observations, surf zone, drifters, near shore circulation			15. NUMBER OF PAGES 59	
			16. PRICE CODE	
17. SECURITY CLASSIFICATION OF REPORT Unclassified	18. SECURITY CLASSIFICATION OF THIS PAGE Unclassified	19. SECURITY CLASSIFICATION OF ABSTRACT Unclassified	20. LIMITATION OF ABSTRACT UU	

NSN 7540-01-280-5500

Standard Form 298 (Rev. 2-89)
Prescribed by ANSI Std. Z39-18

THIS PAGE INTENTIONALLY LEFT BLANK

Approved for public release; distribution is unlimited

LAGRANGIAN OBSERVATIONS OF RIP CURRENTS

Jonathan D. Morrison
Lieutenant, United States Navy
B.S., University of California, Berkeley, 2001

Submitted in partial fulfillment of the
requirements for the degree of

MASTER OF SCIENCE IN PHYSICAL OCEANOGRAPHY

from the

**NAVAL POSTGRADUATE SCHOOL
September 2007**

Author: Jonathan D. Morrison

Approved by: Jamie H. MacMahan
Thesis Advisor

Timothy P. Stanton
Second Reader

Mary L. Bateen
Chairman, Department of Oceanography

THIS PAGE INTENTIONALLY LEFT BLANK

ABSTRACT

A comprehensive field rip-current experiment (RCEX) was conducted from 14 April to 18 May 2007 in Sand City, California, on Monterey Bay. Lagrangian observations were made with inexpensive (\$150), handheld, Differential Global Positioning Systems (DGPS) mounted on surf zone drifters. The inexpensive DGPS requires post-processing to achieve accuracy $O(0.4m)$ and $O(0.01m/s)$. Thirty drifters were constructed and deployed in well-developed, rip-currents to map the circulation patterns for the first time in the field at a high spatial resolution. Drifter observations obtained during three-hour periods on seven different days under varying wave and tidal conditions describe eddies with a rotational period of $4.7min$, confined to the surf-zone and coupled to the rip morphology. On average, three drifters per hour exited the surf-zone. Dependent upon wave conditions, one or two eddies existed between $90m$ -spaced rip-channels, creating a seaward flow in the channels and shoreward flow over the shoals. Cross-shore volumetric flow rates for an alongshore transect through the eddy centers balance to a difference of less than 10% of the gross flow discharge. Velocity measurements obtained from drifter data are evaluated with velocities obtained from stationary, in-situ instruments.

THIS PAGE INTENTIONALLY LEFT BLANK

TABLE OF CONTENTS

I.	INTRODUCTION.....	1
A.	MOTIVATION	1
B.	RIP CURRENT DEFINITION.....	1
C.	HISTORICAL CONTEXT	3
II.	EXPERIMENTAL DESCRIPTION	11
A.	SUMMARY	11
B.	FIELD SITE	11
1.	Site Description	11
2.	Static Array	13
3.	Bathymetric Surveys.....	14
C.	DRIFTERS	15
III.	DATA	17
A.	DATA COLLECTION	17
1.	Method	17
2.	Sources of Error	17
3.	Pre-processing Quality Control	18
B.	DATA PROCESSING	19
1.	Post-processing.....	19
2.	Post-processing Quality Control.....	20
3.	Velocity Binning.....	21
4.	Bathymetric Adjustment.....	23
IV.	RESULTS	25
A.	RIP CHARACTERISTICS.....	25
1.	Rip Currents.....	25
2.	Rip Channels	26
B.	VOLUME BALANCE	27
C.	EDDY CHARACTERISTICS	29
D.	OBSERVATION DENSITY	31
E.	EULERIAN COMPARISON.....	32
V.	CONCLUSIONS	35
A.	SUMMARY	35
1.	General Characteristics.....	35
2.	Drifter Performance	35
3.	Setting the Record Straight.....	36
B.	OTHER WORK	36
1.	Current Research.....	36
2.	Future Research and Improvement	36
3.	Application.....	37
	LIST OF REFERENCES.....	39

INITIAL DISTRIBUTION LIST43

LIST OF FIGURES

Figure 1.	Conceptual representation of a rip current circulation system. Shaded regions represent shoals to either side of a rip channel. Wavy, dotted line represents line of wave breaking. Onshore flow occurs over the shoals. Onshore flow is funneled through feeder channels into the rip channel and seaward as part of the rip current. [After: MacMahan et al., 2005].....	2
Figure 2.	Sketch of a rip current system based on qualitative estimates of flow from early field experiments. [From: Shepard et al., 1941].	4
Figure 3.	Detailed qualitative circulation patterns in the nearshore as determined from field experiments in the 1940s. [From: Shepard and Inman, 1950].....	5
Figure 4.	Flow field derived from measurements in the early 1970s. The seaward flowing rip current can be seen where the streamlines are closest together (center), flanked on either side by shoreward flow with more widely spaced streamlines. [From: Sonu, 1972].	6
Figure 5.	Lagrangian measurements of a rip channel, using floats tracked by two shore-based theodolites. Lack of circulation likely due to rip channel angled obliquely from shore. [From: Brander and Short, 2000].	6
Figure 6.	Quantitative measurements of rip channels, obtained using 10 GPS-tracked surf zone drifters deployed in pairs during five- to six-hour periods. [From: Schmidt et al., 2005].	7
Figure 7.	Mean flow-field from a laboratory tank using monochromatic waves on a barred beach, obtained by moving two instruments from point-to-point. Circulatory patterns are observed with onshore flow over the bars and offshore flow through the channel between adjacent bars. [From: Haller et al., 2002].	8
Figure 8.	(a) Plan view of field site used for the Rip Current Experiment (RCEX). (b) Close-up of field site with sign warning bathers about submerged equipment.	11
Figure 9.	Cross-shore bathymetric profile over the shoal at the site. Zero datum in elevation corresponds to mean sea level for 4 May 2007. Cross-shore coordinates show meters from experimental origin rather than meters from shoreline.	12
Figure 10.	Static array and site bathymetry. X-axis is alongshore direction and positive to the left. Y-axis is cross-shore direction and positive up. Red dots represent in situ instruments and are plotted in the local coordinate system against bathymetry typical of the field site. Mean shoreline is the border between blue contours (submerged bathymetry) and yellow contours (exposed beach).	13
Figure 11.	Static array plotted against bathymetric surveys from: (a) 22 Apr, (b) 1 May, (c) 11 May, and (d) 18 May 2007. Spikes in bathymetry (11 and 18 May) are caused by noise. Note consistent rip channel locations between surveys.	14
Figure 12.	Detailed diagram of drifter construction.	16

Figure 13.	Unfiltered time-series data for a single drifter on 5 May 07: (a) unfiltered cross-shore position; (b) unfiltered cross-shore velocity. Time series are mostly smooth, but noise in the positional time-series results in a noisy velocity time-series.	20
Figure 14.	Time-series data after quality control, for the same drifter as Figure 13: (a) cross-shore position; (b) cross-shore velocity. Smoothness is significantly improved after filtering.	21
Figure 15.	Bin-averaged velocity vectors plotted against bathymetry using: (a) $5m \times 5m$ grid spacing; and (b) $10m \times 10m$ grid spacing. The average shoreline for the deployment period is represented by the border between yellow contours (sand) and blue contours (water). Arrows are vectors of averaged velocities within each bin. Vectors shoreward of the shoreline are the result of tidal changes in the mean-water level during the deployment and possibly from imperfect removal of points during quality control. The smaller bin size provides finer resolution, but introduces more noise, while the larger bins provide smoother profiles at the expense of slightly lower resolution.	22
Figure 16.	Cross-shore velocities in a rip channel. Cross-shore axis is normalized for the experiment to represent meters from the shoreline rather than meters from the local coordinate system alongshore axis.	25
Figure 17.	Cross-shore bathymetric profile in a rip channel. Cross-shore axis is normalized for the experiment to represent meters from the shoreline rather than meters from the local coordinate system alongshore axis.	26
Figure 18.	Alongshore bathymetric profile $\sim 50m$ from the shoreline, showing how rip-channel spacing and width were determined.	27
Figure 19.	Alongshore profile of cross-shore velocities $\sim 50m$ from the shoreline. Positive velocities are off-shore, while negative velocities are onshore.	28
Figure 20.	Volumetric flow rate profiles along transect located $\sim 50m$ from the shoreline – positive is offshore flow.	29
Figure 21.	Sample autocorrelation plot of cross-shore positions. Lag (seconds) is the x-axis and auto-correlation value (m^2) is the y-axis. Since the auto-correlation is based on demeaned and detrended data, the peak at zero lag represents the square of the data variance. The value of lag at the next peak in auto-correlation corresponds to the period of oscillation for the data set.	30
Figure 22.	Observation density plot, showing higher concentration of drifter observations at the centers of surf zone eddies.	32
Figure 23.	Results of a linear regression comparing average in situ instrument velocities with average drifter velocities near them. While there is scatter in the data correlation is relatively high (r-squared of 0.81,) with a best fit slope just less than one, and y-intercept only slightly larger than zero.	33

LIST OF TABLES

Table 1.	Eddy characteristics for the six deployment days with any observed eddies. The “overall” average excludes measurements from 10 May and 15 May – even though eddies were observed on those days, flow was primarily alongshore.	31
----------	---	----

THIS PAGE INTENTIONALLY LEFT BLANK

ACKNOWLEDGMENTS

I would like to thank Rob Wyland, Keith Wyckoff, Ron Cowen, James Stockel, Mark Orzech, Nick Dodd, and Petty Officer Huynh for their countless lab and field hours building and installing the equipment we used in the RCEX. I would also like to thank Ed Thornton, Tim Stanton, Edie Gallagher, and Ad Reniers for the combined years of Oceanographic expertise they shared with me during the experiment and during my time here at the Naval Postgraduate School. Thanks to Jeff Brown and Jenna Brown from the University of Delaware, Martijn Henriquez from Delft University, and LT Natalie Laudier from our own Oceanography Department for their help collecting and analyzing data required for the numerous aspects of this puzzle. I thank my advisor Professor Jamie MacMahan for his patience with the steep learning curve we both faced here at NPS, for challenging me to complete my thesis within six months, and for his involvement to ensure I had the tools to do so. Most importantly, I'd like to thank my family for their patience with my physical (and sometimes mental) absence – especially my fiancée, Danielle, for putting up with my frustrated late nights and grouchy early mornings, and supporting me with her faith that I could do it and her positive attitude despite the challenges she has faced as a new sixth-grade teacher.

THIS PAGE INTENTIONALLY LEFT BLANK

I. INTRODUCTION

A. MOTIVATION

The ocean has potential to both give life and take it away, especially near shore. According to the United States Lifesaving Association (USLA), 100 deaths occur annually due to rip currents, and 80% of all beach lifeguard rescues are rip current related (USLA, 2007). There is a great amount of interest in surf zone circulation with a wide variety of applications, including sediment and pollution transport, shoreline evolution, and beach and swimmer safety. Furthermore, research focused on rip currents is important in predictive surf zone modeling that ultimately aids military planners in mine-hunting and SEAL delivery.

Rip currents are typically “shore-normal, narrow, seaward-flowing currents” that extend from the shoreline to the edge of the surf zone with relatively high speeds (MacMahan et al., 2005). Since the 1930s, field experiments have collectively improved our understanding of rip current dynamics (Shepard et al., 1941; Shepard and Inman, 1950; Sonu, 1972; Brander, 1999; Brander and Short, 2000; Schmidt et al., 2005; MacMahan et al., 2005). Owing to the cost, difficulty, and danger of installing multiple instruments throughout a rip current system many hypotheses remain unanswered. Lagrangian observations have, for the most part, qualitatively complemented Eulerian measurements, and have the potential to resolve these rip current hypotheses. Until now, the cost of accurate drifter measurements has limited the numbers deployed, and therefore our ability to quantitatively understand rip current systems. The goal of this thesis is to transform previously qualitative Lagrangian descriptions of rip currents into a more quantitative description, using a fleet of inexpensive, accurate, self-logging drifters recently deployed in the field.

B. RIP CURRENT DEFINITION

A rip current can essentially be thought of as a localized river in the ocean, carrying water from the shoreline out to sea. Differences in bathymetry lead to variations

in wave breaking along shore that cause a higher mean water level over shoals than over rip channels. The resulting circulation pattern (Figure 1) is offshore-directed flow in the rip channel and onshore flow over the shoals to either side.

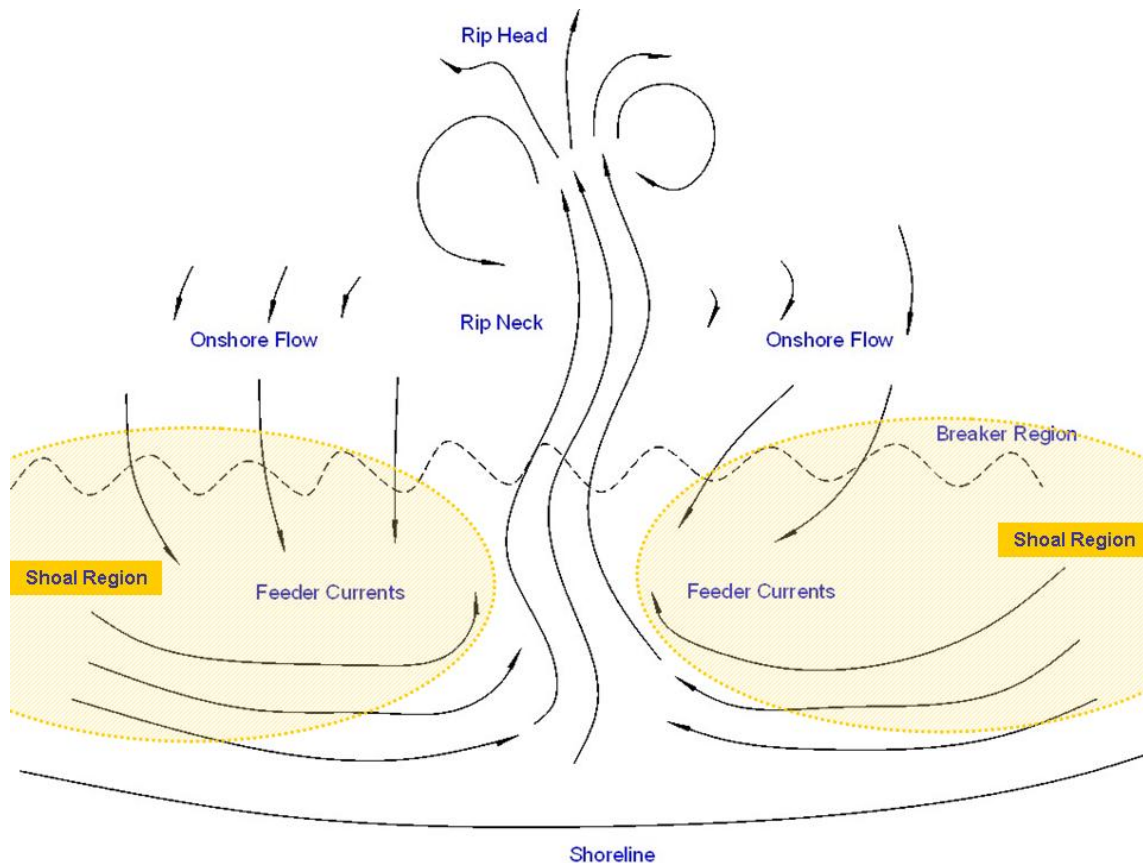


Figure 1. Conceptual representation of a rip current circulation system. Shaded regions represent shoals to either side of a rip channel. Wavy, dotted line represents line of wave breaking. Onshore flow occurs over the shoals. Onshore flow is funneled through feeder channels into the rip channel and seaward as part of the rip current. [After: MacMahan et al., 2005].

A conceptual drawing illustrates the primary aspects of a rip current cell (Figure 1). The dotted line represents wave breaking – $O(100m)$ from the shoreline in the recent rip current experiment (RCEx), but this is dependent on wave and tide conditions. When most beach-goers describe rip currents, they think of the rip neck, the narrowest section of the rip characterized by strong seaward flow. The rip head is the seaward tip of the rip, where rip currents diffuse and lower velocities are present. The flow in the rip head

is less constrained by bathymetry of the rip channel and spreads laterally. Returning onshore flow is funneled into the rip through alongshore-directed feeder currents, which occur near the shoreline.

In 1941, Shepard et al., showed the intensity of rip currents increases with increasing wave height and observed a similar trend in their seaward extent. From this they concluded that rip currents result from wave translational motion piling up along the shoreline, which must return offshore to satisfy continuity. Some of the returning water is concentrated in zones, which develop in persistent outward currents, called rip currents. This hypothesis and several others have been proposed to explain the formation of rip currents.

Other potential mechanisms for rip current generation have been separated into two main categories: wave interaction and structural (boundary) interaction (Dalrymple, 1978). The wave interaction theories suggest that rip currents are caused and strengthened by variations in mean water level along the shore leading to hydrostatic differences. Such theories include: interaction between incident edge waves (traveling along the shore) (Bowen, 1969; Bowen and Inman, 1969); intersecting wave trains (Dalrymple, 1975); or wave-current interaction (LeBlond and Tang, 1974; Dalrymple and Lozano, 1978). Boundary interaction theories suggest that rip currents are the result of circulation patterns created by wave field interaction with topographical variations, such as bathymetry (Bowen, 1969; Noda, 1974; Dalrymple et al., 1976) or artificial structures (Liu and Mei, 1976; Mei and Angelides, 1977) – e.g. jetties. Problems with these theories were that the former under-predicted surf zone energy dissipation, while the latter failed to accurately predict the wave field over longshore sand bars (Dalrymple, 1978).

C. HISTORICAL CONTEXT

Surf zone circulation and dynamics have been studied for several decades, and interest in rip currents can be traced back to the mid-1930s when a scientific debate about the existence of an “undertow” led Shepard (1936) to coin the term “rip current” as a descriptive name for the phenomenon that seemed to vex lifeguards. Subsequent

research has shown that undertow does exist (Hansen and Svendsen, 1984), but occurs on two-dimensional beaches rather than three-dimensional beaches where rip currents are the norm.

Early experiments were primarily qualitative, visually tracking dye, wave breaking patterns, kelp, and other floating objects (Shepard, 1936; Shepard et al., 1941; Shepard and Inman, 1950). Rip currents in these studies were characterized by velocities from 9cm/s - 22cm/s (Shepard et al., 1941); widths from $15\text{-}150\text{m}$ and offshore extents from $100\text{-}800\text{m}$ (Shepard, 1936; Shepard et al., 1941); and spacing $O(180\text{m})$. These early studies generalized nearshore circulation as net shoreward flow in wide lanes between seaward flowing rip currents (Shepard and Inman, 1950) and permitted qualitative representations of nearshore flow (Figures 2 and 3).

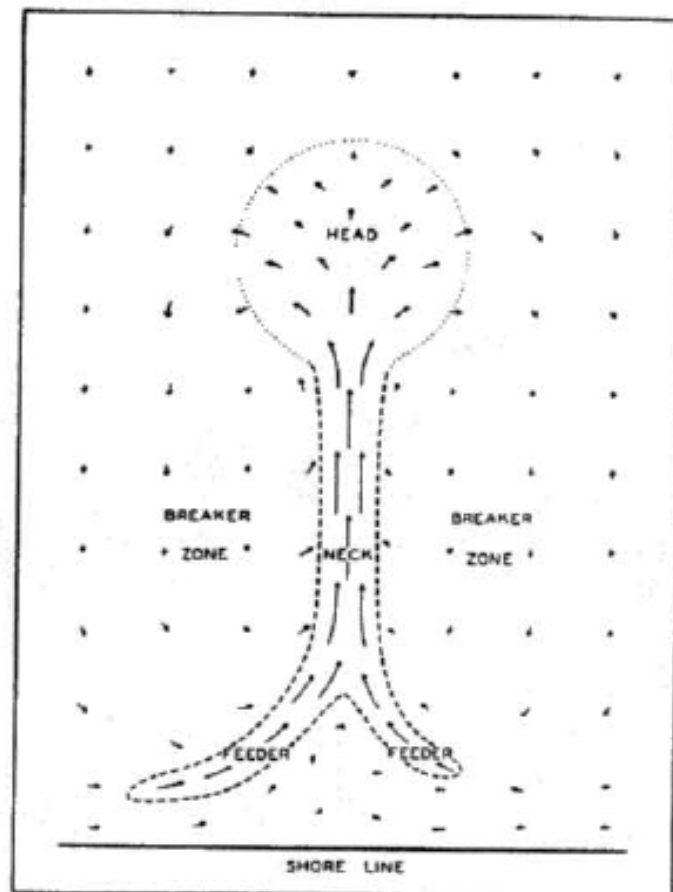


Figure 2. Sketch of a rip current system based on qualitative estimates of flow from early field experiments. [From: Shepard et al., 1941].

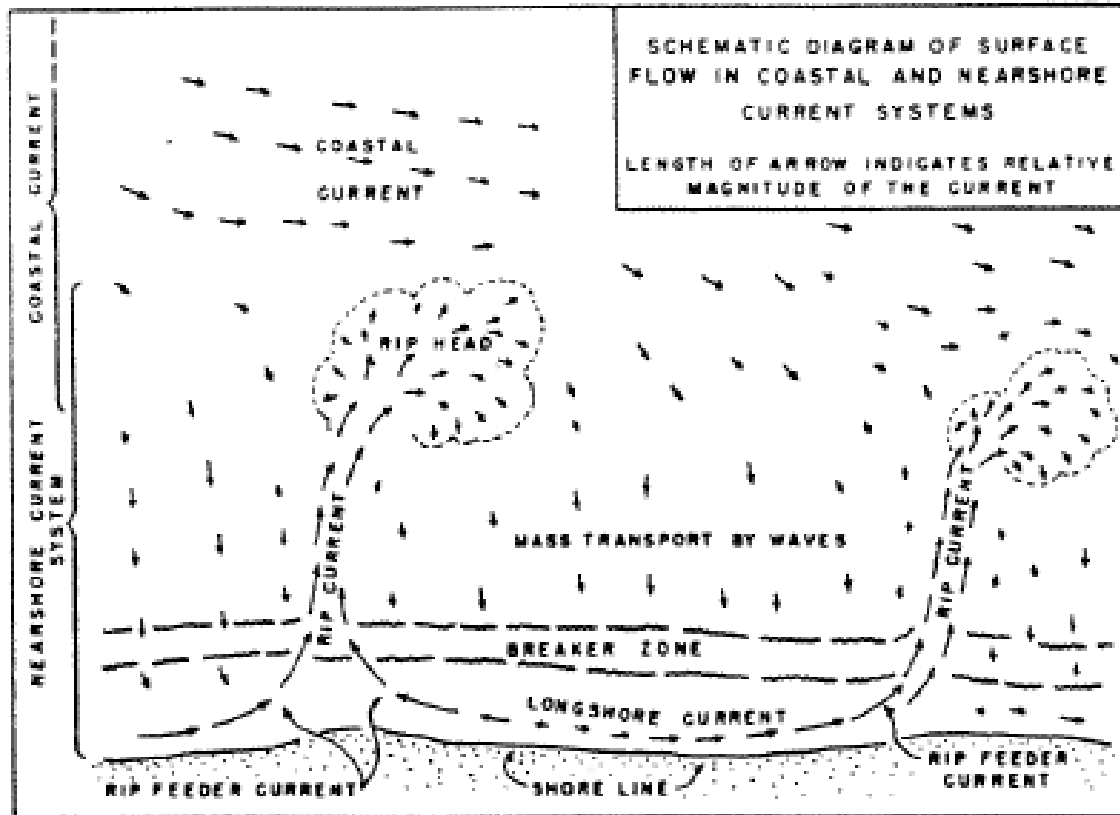


Figure 3. Detailed qualitative circulation patterns in the nearshore as determined from field experiments in the 1940s. [From: Shepard and Inman, 1950].

Later experiments compared visually derived measurements with measurements from static instruments in the rip channels and on the shoals (Sonu, 1972; Brander and Short, 2000). These experiments provided more quantitative pictures of surf zone circulation (Figures 4 and 5). Circulation was characterized by mean rip current velocities $O(60-70\text{cm/s})$ (Sonu, 1972; Brander and Short 2000), with a maximum as high as 2m/s (Sonu, 1972), and onshore flow between rip currents from $20-30\text{cm/s}$ (Sonu, 1972).

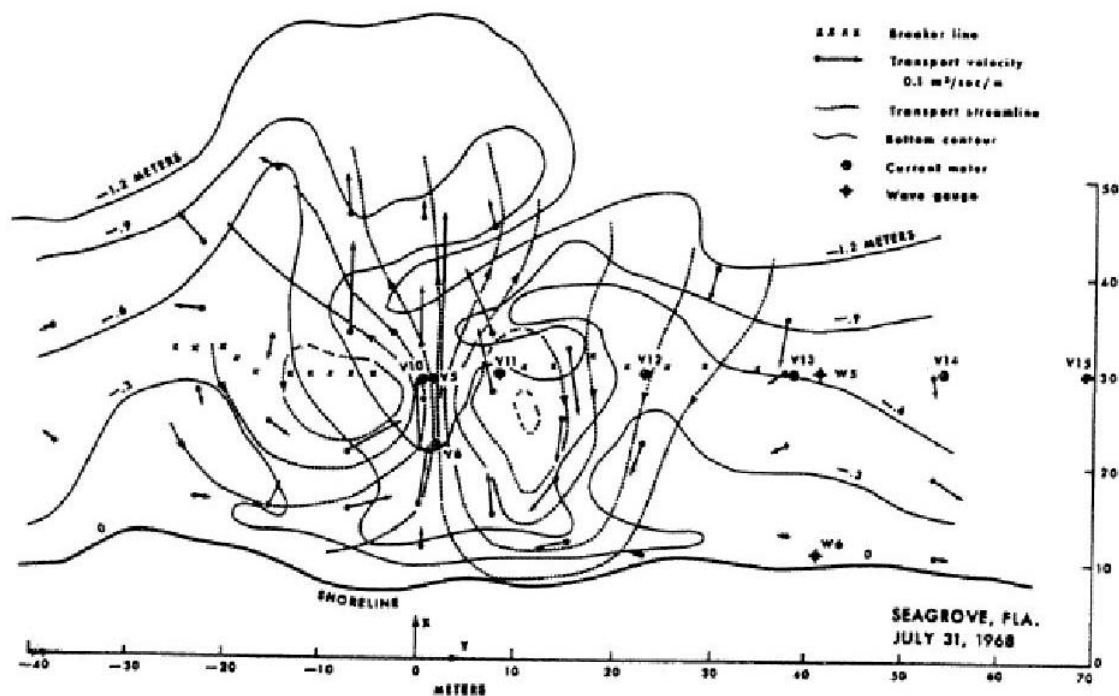


Figure 4. Flow field derived from measurements in the early 1970s. The seaward flowing rip current can be seen where the streamlines are closest together (center), flanked on either side by shoreward flow with more widely spaced streamlines. [From: Sonu, 1972].

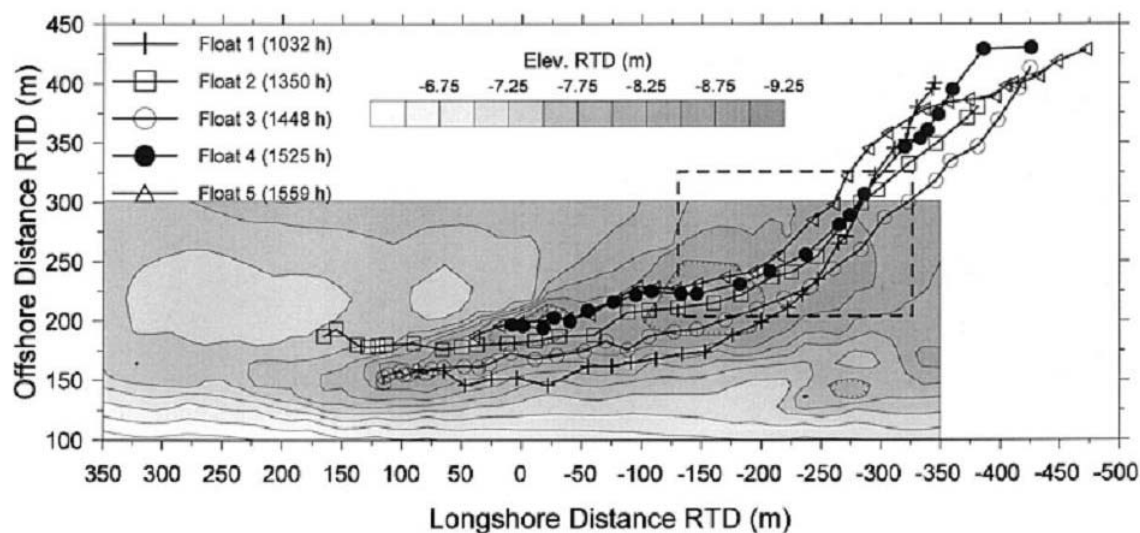


Figure 5. Lagrangian measurements of a rip channel, using floats tracked by two shore-based theodolites. Lack of circulation likely due to rip channel angled obliquely from shore. [From: Brander and Short, 2000].

More recently, Global Positioning System (GPS)-tracked drifters have further improved our understanding of the surf zone (Schmidt et al., 2005), to show rip current intensification as tide level decreases. Unfortunately, owing to the high cost, O(\$6K), of these systems, only 10 drifters were used, and drifters were only released in pairs, providing a limited physical picture of the flow structure (Figure 6).

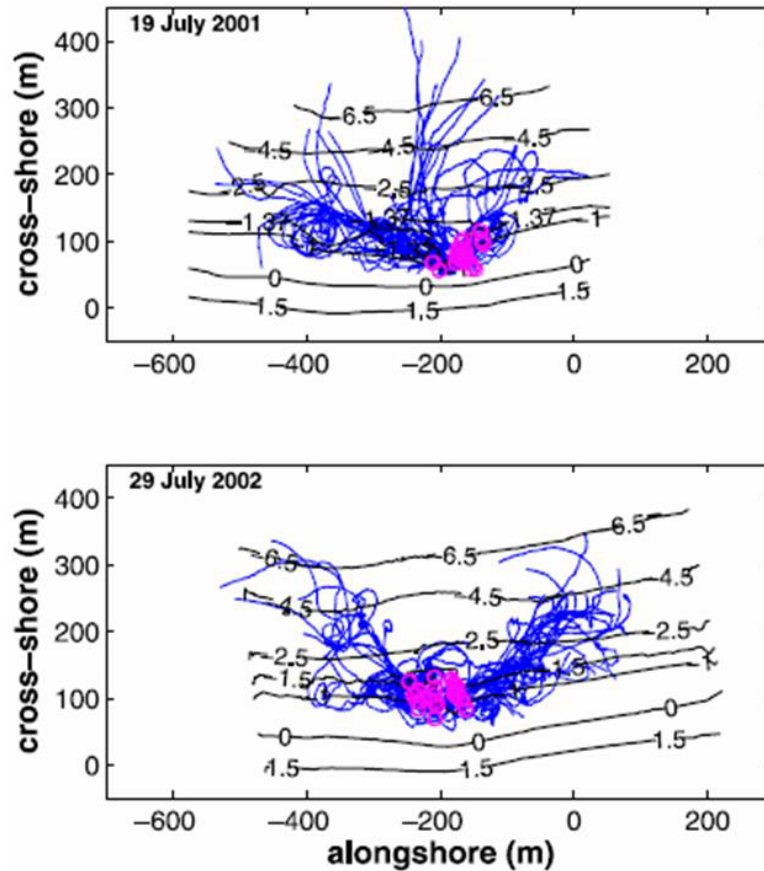


Figure 6. Quantitative measurements of rip channels, obtained using 10 GPS-tracked surf zone drifters deployed in pairs during five- to six-hour periods. [From: Schmidt et al., 2005].

Recent laboratory experiments using Acoustic Doppler Velocimeters (ADV) to measure current patterns on a barred beach with rip channels suggest that bars and rip channels dominate nearshore dynamics (Haller et al., 2002). These results provide good physical detail and show distinct eddies with offshore flow over rip channels and onshore

flow over adjacent shoals (Figure 7). However, the laboratory conditions used in this experiment do not accurately reflect field conditions, since the waves were monochromatic (Haller et al., 2002). Laboratory experiments often use a smaller scale than field conditions, and are thus limited in their ability to reproduce realistic conditions. Additionally, laboratory results are often difficult to reproduce under realistic field conditions, owing to the cost and difficulty of placing such a large array in the field.

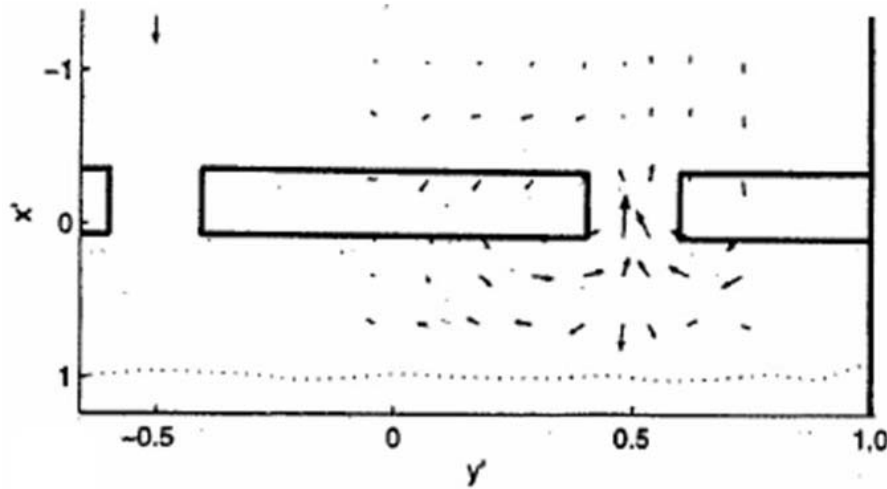


Figure 7. Mean flow-field from a laboratory tank using monochromatic waves on a barred beach, obtained by moving two instruments from point-to-point. Circulatory patterns are observed with onshore flow over the bars and offshore flow through the channel between adjacent bars. [From: Haller et al., 2002].

While the numerical results focusing on rip currents have certainly increased our understanding of surf zone circulation, the results are largely evaluated at a limited number of fixed instrument arrays that have not captured the full development of rip current circulation cells. Until recently, the scarcity of Lagrangian data has meant Eulerian measurements have been the primary data available for predictive surf zone modeling (Johnson and Pattiaratchi, 2004).

Furthermore, owing to the high cost of GPS-tracked surf zone drifters, most Lagrangian observations have taken place in the laboratory under ideal bathymetric conditions (Kennedy and Thomas, 2004), and those that have taken place in the field

have been limited in size (Schmidt et al., 2005). Recently, an inexpensive (~\$150) hand-held GPS device was tested for use in oceanographic drifters (MacMahan and Brown, 2007). The positive results of these tests permitted construction of a larger fleet of drifters (30 drifters) for the 2007 rip current experiment (RCEX) at a significantly lower cost, without sacrificing precision.

THIS PAGE INTENTIONALLY LEFT BLANK

II. EXPERIMENTAL DESCRIPTION

A. SUMMARY

A field rip-current experiment (RCEX) was conducted from 14 April to 18 May 2007 to examine rip-current circulation patterns in greater detail. Eulerian measurements were obtained using a stationary array of 11 instruments. Lagrangian measurements were obtained with 30 inexpensive drifters.

B. FIELD SITE

1. Site Description

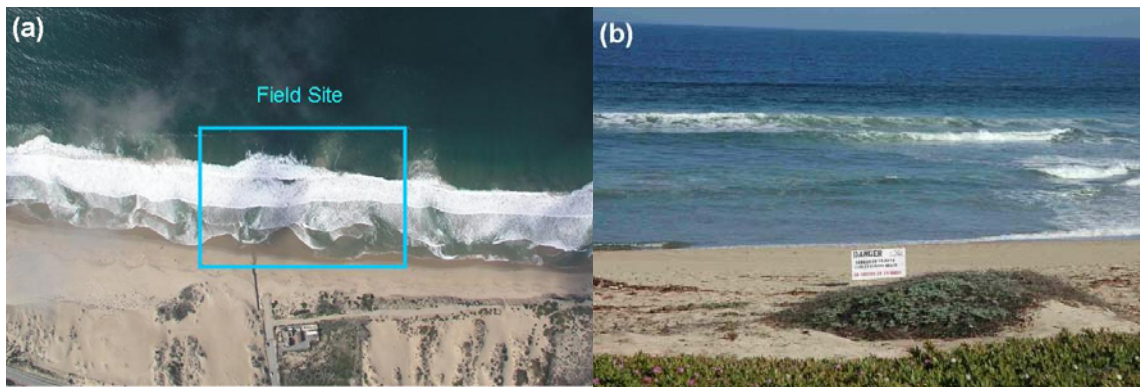


Figure 8. (a) Plan view of field site used for the Rip Current Experiment (RCEX).
(b) Close-up of field site with sign warning bathers about submerged equipment.

The field site was approximately a 300m alongshore by 250m cross-shore region located in Sand City, California, at the south end of the Monterey Bay (Figure 8).

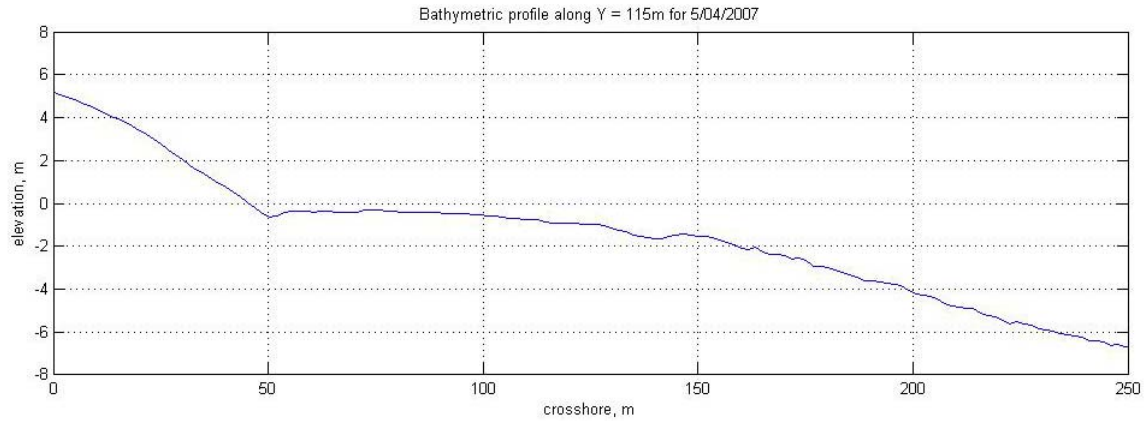


Figure 9. Cross-shore bathymetric profile over the shoal at the site. Zero datum in elevation corresponds to mean sea level for 4 May 2007. Cross-shore coordinates show meters from experimental origin rather than meters from shoreline.

This is the same site used in the 2001 RIPEX experiment and is characterized by shore-normal waves, coarse sand, and persistent, energetic rip currents (MacMahan, et al., 2005). The beach foreshore is steep (1:9), with a low-tide terrace (1:100), and an offshore slope of 1:20 (Figure 9).

For consistency, the local coordinate system is also based on RIPEX coordinates (MacMahan, et al, 2005). The mean shoreline (zero vertical-axis datum level) is about 50m from the origin, and parallel with the alongshore component of the array. Positive is toward the North and offshore.

2. Static Array

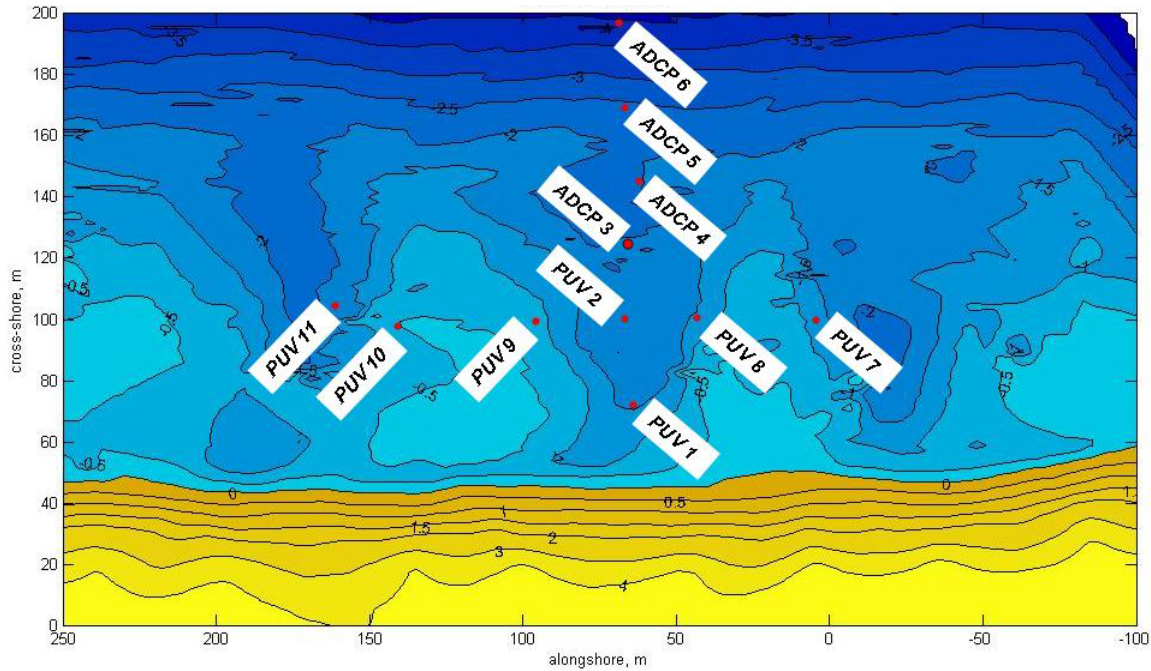


Figure 10. Static array and site bathymetry. X-axis is alongshore direction and positive to the left. Y-axis is cross-shore direction and positive up. Red dots represent in situ instruments and are plotted in the local coordinate system against bathymetry typical of the field site. Mean shoreline is the border between blue contours (submerged bathymetry) and yellow contours (exposed beach).

The stationary array comprised of an intersecting alongshore-cross-shore array (Figure 10). The alongshore array consisted of seven digital electromagnetic current meters co-located with pressure sensors (PUVs) mounted on 10-foot poles that were air-jetted approximately seven feet into the seabed. The cross-shore component of the array consisted primarily of Acoustic Doppler Current Profilers (ADCPs) mounted on 10-foot poles jetted into the bed approximately five feet, deployed down the center of the main rip channel. The instruments were inspected every couple of days, cleared of sand and kelp, and raised or lowered as necessary, in order to ensure continuity and consistency of measurements. These observations were part of RCEX, but are not the focus of this thesis.

3. Bathymetric Surveys

Three different types of sub-aerial and sub-aqueous surveys were performed as part of the experiment to capture morphologic changes. Large spatial extent surveys of the beach face were performed using an All-Terrain Vehicle (ATV) during low tide on 15 March and 9 May 2007. A wave-rider (personal watercraft, PWC) was used for bathymetric surveys of the site (from inside the surf zone to 200m from the shoreline) during high tide on 20 March, 21 April, and 1, 11, and 18 May 2007. The presence of waves and bubbles inside the surf zone made it difficult to obtain measurements by PWC alone. Walking surveys of the beach face and shoals at the field site were also conducted during low tide on 20 March, 19, 22, and 23 April, and 2, 8, 11, and 18 May 2007. Additionally, the instrument locations were surveyed on 22 April, and 11 and 18 May 2007. A total of four complete surveys, and three instrument location surveys were performed. The combined ATV, PWC, and walking surveys overlapped enough to provide a good picture of beach and surf zone morphology in the area of interest.

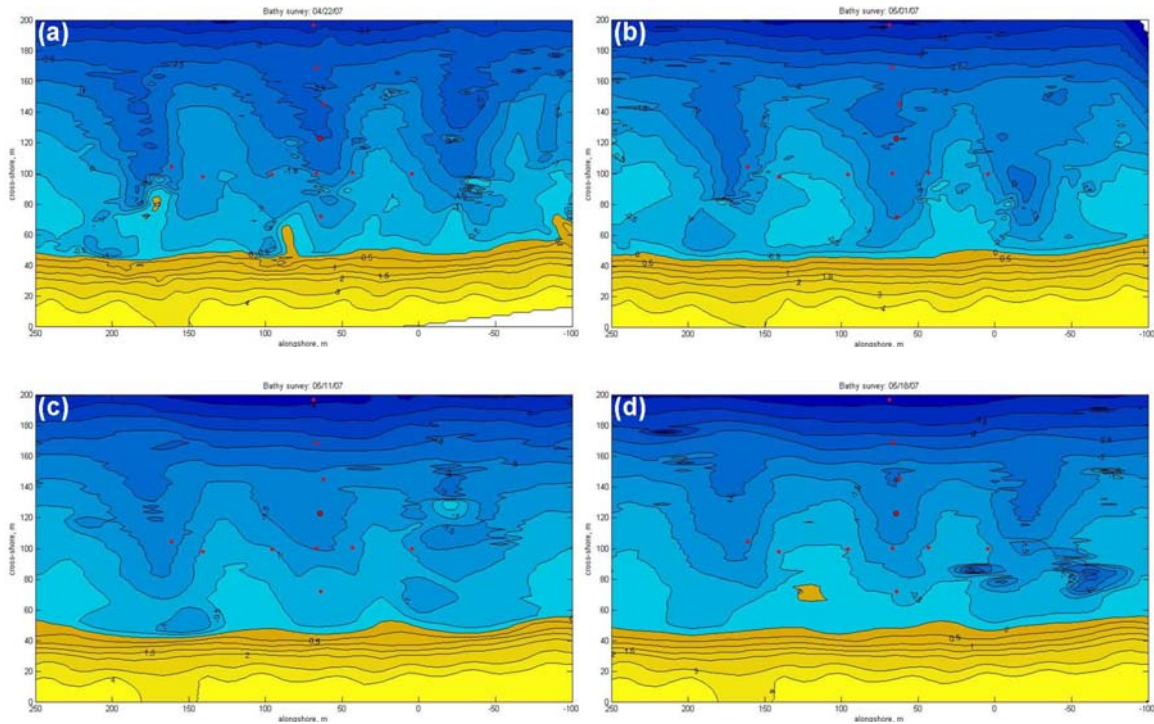


Figure 11. Static array plotted against bathymetric surveys from: (a) 22 Apr, (b) 1 May, (c) 11 May, and (d) 18 May 2007. Spikes in bathymetry (11 and 18 May) are caused by noise. Note consistent rip channel locations between surveys.

To simplify calculations, an assumption is made that bathymetry does not change significantly between bathymetric surveys. There is very little change in the bathymetry over the course of several surveys (Figure 15), demonstrating the validity of this assumption. Consequently, depth is approximated for any point at the field site given the most recent bathymetric survey by accounting for mean sea level measured during each deployment. This process is later described in detail.

C. DRIFTERS

Surf zone drifters have been used in research for decades – even volleyballs and kelp used in early experiments are technically drifters (Shepard, et al., 1941; Shepard and Inman, 1950). Advances in technology permitted installation of small GPS receivers on drifters that have improved measurement accuracy (Johnson, et al., 2003; Schmidt, et al., 2003; Schmidt, et al., 2005). The high cost of commercially available drifters using this technology has made it difficult to obtain more than 10 for any experiment and unpleasant to risk loss of any, resulting in limited detail (Schmidt, et al., 2005). Less expensive drifters O(\$500) have been built at the expense of either reduced accuracy or a time-consuming process to match the accuracy of those available commercially (Johnson, et al., 2003).

The focus of this research effort was an inexpensive drifter designed to use handheld, off-the-shelf Differential GPS (DGPS) technology. MacMahan and Brown (2007) modified a commercially available DGPS logger O(\$150) to obtain system accuracy O(0.4m) in position and O(0.01m/s) for velocity after post-processing. The low cost (less than \$250 each without labor) of the drifters built with this technology allowed construction of a fleet of 30, for about the same cost as a single commercially available drifter. The large number of drifters permitted data collection with greater spatial and temporal resolution than achieved by previous studies.

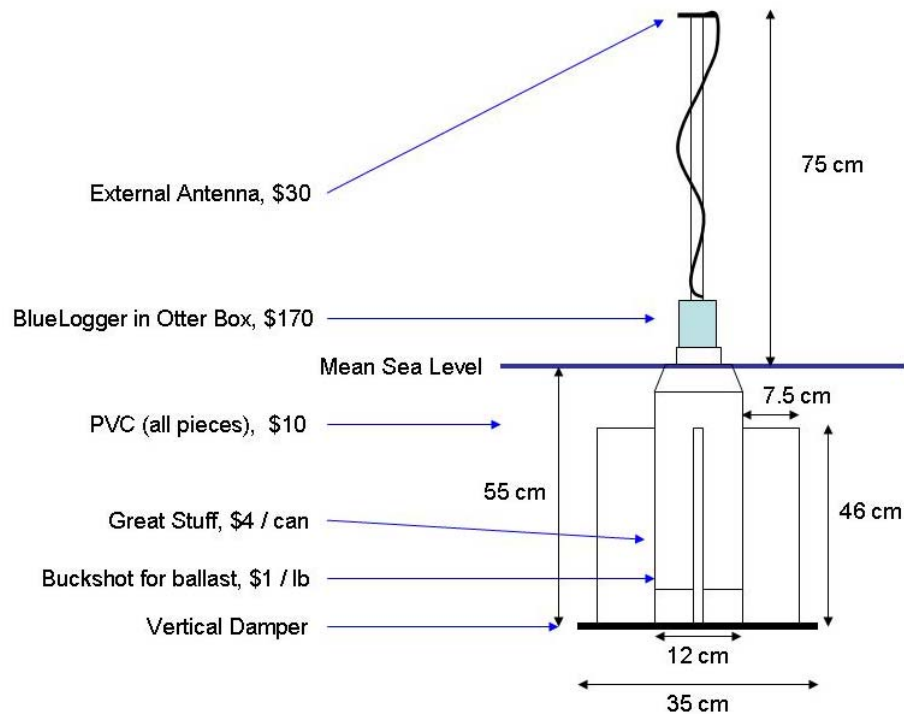


Figure 12. Detailed diagram of drifter construction.

Figure 12 is a graphical representation of a drifter. The drifter body designed for this experiment is a 55cm length of PVC pipe with an outer diameter of 12cm, and is surmounted by a 75cm antenna pole of PVC pipe with an outer diameter of 2.6cm – for an overall height of 1.3m. A 35cm-dia. disk of PVC is attached to the bottom of the body to dampen vertical motion, and 27cm-dia. octagonal, stainless steel plate is attached to the bottom of that to add structural integrity and improve the drifter’s righting moment. Three fins (46cm tall by 7.5cm wide) are equally spaced around the body to improve it’s flow response. The body is filled with enough buckshot to give the drifter its desired draft and improve its righting moment, and expanding foam is added inside to prevent the buckshot ballast from shifting. A water-proof case is attached to the bottom of the antenna pole to house the DGPS logger, and an external antenna is mounted on top of the antenna pole. The total price tag of \$250 per drifter (without labor) includes: the DGPS logger, external antenna, waterproof box, PVC to build the drifter, enough buckshot for ballast, and expanding foam to stabilize the buckshot.

III. DATA

A. DATA COLLECTION

1. Method

To collect Lagrangian data, drifters were deployed on seven days: 27 April, and 4, 5, 7, 10, 15 and 19 May 2007. Deployment periods lasted from approximately 0830 to 1200 on each day. On a given deployment day, five or six people would initially start loggers for 10 to 12 drifters. Once the lights of the loggers were flashing, to indicate they were collecting data, the drifters were taken to the water, and deployed as close to each other as possible without their bodies interfering with each other. As soon as the first group of drifters were released in the surf zone, another group of 10 to 12 would similarly be started and deployed. Drifters were removed from the water when they started to drag along shoals or when they left the boundaries of the observational domain. Drifters that left the surf zone offshore were picked up by boat and turned off for the day. Throughout the deployment period drifters were deployed in similar-sized groups composed of new drifters and/or those that washed up on shore or crossed the longshore boundaries. At one point, as many as 25 drifters were simultaneously circulating in the surf zone. At the end of the day, logged data were uploaded to computer for post-processing, and data were cleared from the loggers for the next deployment.

Data from the stationary array were used for comparison to evaluate flow.

2. Sources of Error

There were several sources of error introduced to the data during collection. Generally the easiest to identify was human influence on the drifters. Since the logging devices were turned on before the drifters were taken to the water, there were a few minutes of positional data at the beginning of each set that had nothing to do with the flow field. The same is true whenever drifters were removed from the water.

Additionally, drifters would occasionally become trapped on shoals or shoreline close enough to a rip current that it was given a push to set it back in the current. Times of occurrence were recorded by a note-taker.

Another source of error was drifter entanglement in kelp. Floating kelp bodies attached to a drifter would unfavorably bias drifter speeds and had to be removed as soon as possible. Since bodies of floating kelp were fairly large, it was generally easy to identify when they entangled a drifter. When drifter entanglement was noticed, a swimmer would remove the kelp from drifter as soon as practicable, and the entanglement and disentanglement times were recorded by a note-taker.

Perhaps the most difficult sources of error to identify were breaking waves. While the drifters are designed to prevent excessive vertical oscillations due to waves (fins and a vertical damper), breaking waves affected the drifters by occasionally submerging their antennas. Drifters were designed to pass under oncoming waves (to prevent surfing) and their signal was periodically interrupted or degraded when this occurred. Also, during the first deployment waves knocked the external antennas from their plates on top of the antenna poles.

3. Pre-processing Quality Control

To mitigate sources of error as best as possible we implemented several methods of quality control. To prevent waves from knocking antennas from drifters after the first deployment, the external antenna was glued to the top of the antenna plate using epoxy.

To minimize the error introduced by human interaction with the data, efforts were made to devise a way to turn the logging devices on and off without opening the waterproof boxes while the drifters were carried by people. These efforts were unsuccessful. However, it was recognized that isolating the external antenna from the satellite signal would prevent the loggers from recording data and achieve the same result. Caps were designed to cover the external antenna that successfully isolated the signal. However, the caps proved cumbersome in the surf zone, and were rarely used.

For each deployment, boundaries were established outside of which we would retrieve the drifters and discount data. If drifters were retrieved inside of those boundaries we made every effort to move quickly up the beach past high water to make it obvious that motion on the remainder of that track was not the result of currents. When drifters exited the surf zone they were retrieved by boat. Since the boat would occasionally move at slow speeds that could be mistaken for currents, drifter tracks were also truncated once they left the surf zone.

Ultimately, a note-taker proved to be key for quality control. The note-taker was responsible for recording: time each logger was started and stopped; time each drifter entered the water, was removed from the water, or exceeded observation boundaries; time each drifter became tangled or untangled from kelp; and (during the first deployment) time each drifter antenna was knocked off by a wave and replaced by swimmers. During deployments the note-taker had no other responsibilities due to the importance of the job. Since it would be difficult for one person to keep track of so many drifters, those deploying drifters helped the note-taker by reporting observations of any of the listed occurrences to the note-taker.

B. DATA PROCESSING

1. Post-processing

The DGPS data collected by the drifters were uploaded from drifter and base station logging devices and post-processed using commercial software. Since the base station was stationary, an estimate of the pseudo-range bias (difference between actual and measured distance between GPS satellite and receiver, based on upper-atmosphere effects) was calculated for each data point from the base station (MacMahan and Brown, 2007). Since the base station and drifter antennas were in close proximity, the same upper-atmospheric conditions affect them, and the base station bias for each data point was removed from the drifter-logged for each corresponding time. Position errors using non-differential GPS are on the order of 10m. Use of DGPS reduces that error to the order of centimeters (MacMahan and Brown, 2007). Processed logger files were converted to text format.

Drifter positions were recorded every two seconds. In order to make the positions more meaningful, the global Universal Transverse Mercator (UTM) coordinates for each observation were first transformed to local RCEX coordinates. Corresponding u - and v -components of velocity are calculated by a forward differencing scheme.

2. Post-processing Quality Control

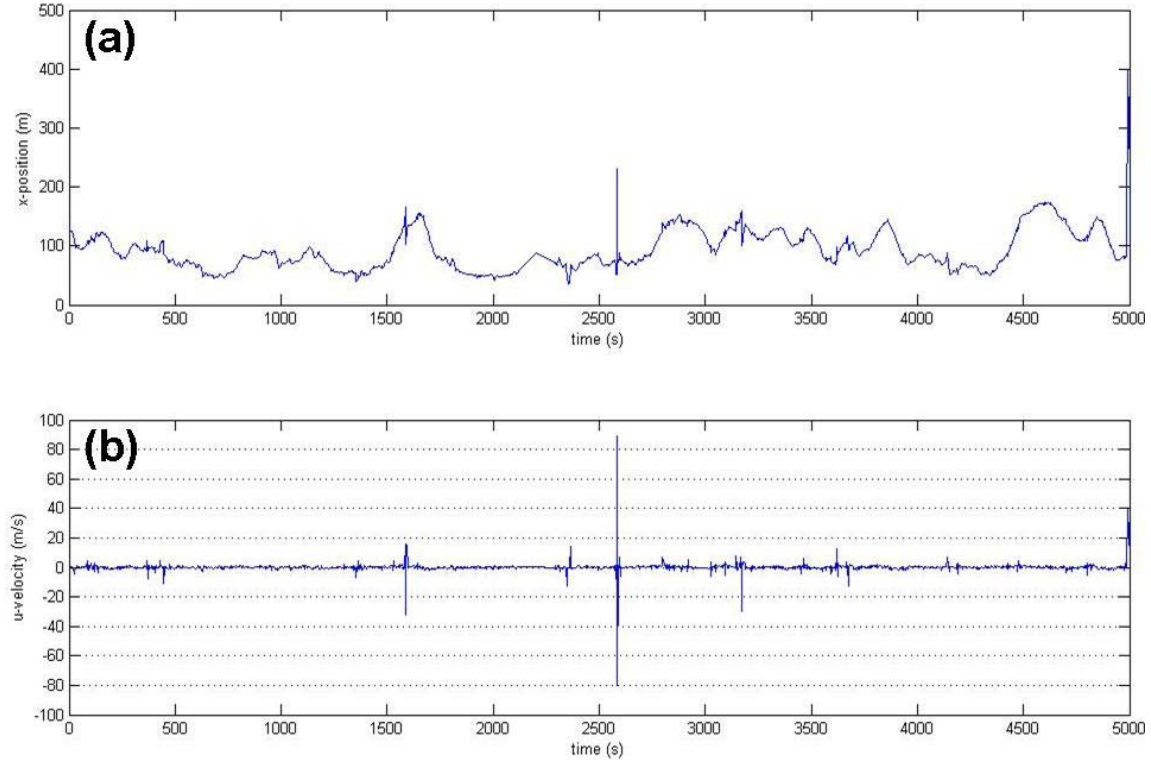


Figure 13. Unfiltered time-series data for a single drifter on 5 May 07: (a) unfiltered cross-shore position; (b) unfiltered cross-shore velocity. Time series are mostly smooth, but noise in the positional time-series results in a noisy velocity time-series.

Once the data were in local coordinates and time, deployment notes were used to remove human- and kelp-influenced data. The resulting time-series (Figure 13) were overall smooth, but still had obviously erroneous spikes in position and hence velocity. To remove the spikes, the data were filtered by removing outliers that were greater than three standard deviations from the mean velocity for that drifter deployment. After

filtering twice data were visually checked and points were individually removed if they met velocity criteria but still exceeded reasonable spatial separation.

The resulting gaps in position data are filled using a spline interpolation for gaps of 10s or less, and linear interpolation for larger gaps. The resulting data are much smoother than before the quality control process. (Figure 14)

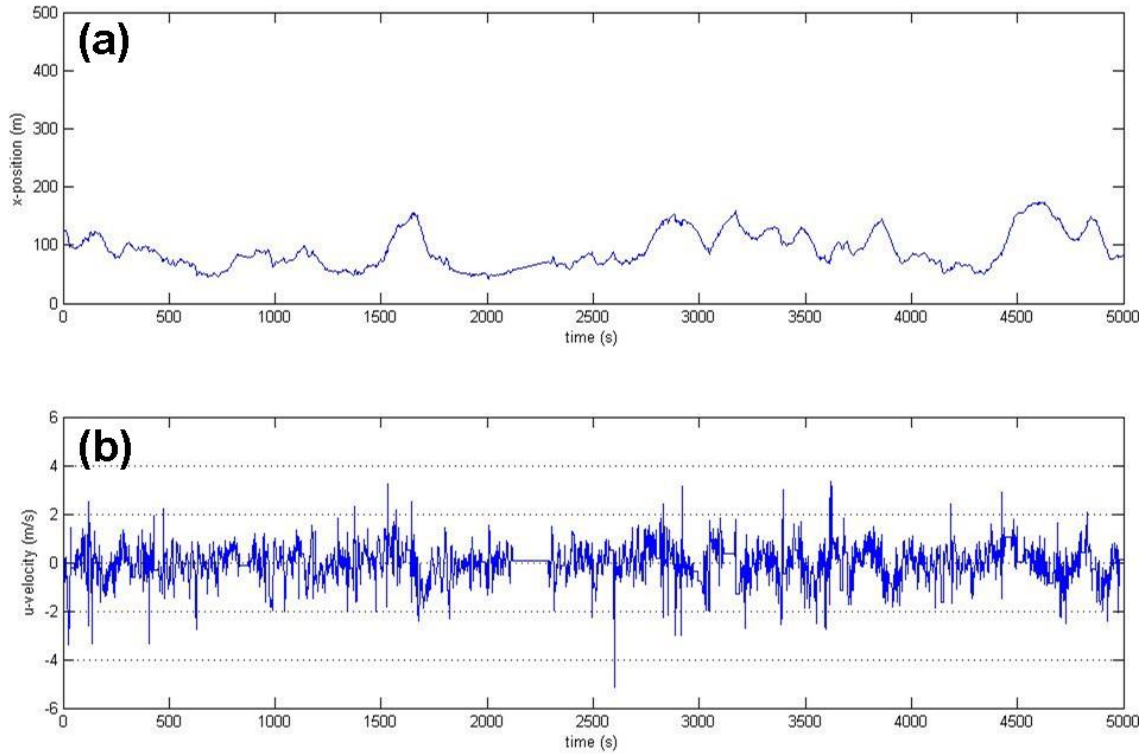


Figure 14. Time-series data after quality control, for the same drifter as Figure 13: (a) cross-shore position; (b) cross-shore velocity. Smoothness is significantly improved after filtering.

3. Velocity Binning

The u- and v-components of velocity are grouped by dividing the field site into a spatial grids on $5m \times 5m$ and $10m \times 10m$ bins for comparison. The means and standard deviations of the velocity components are calculated for each bin. Velocity averages are then plotted as vectors against a background of bathymetric contours to show a qualitative relationship between the flow pattern and bathymetry (Figure 15).

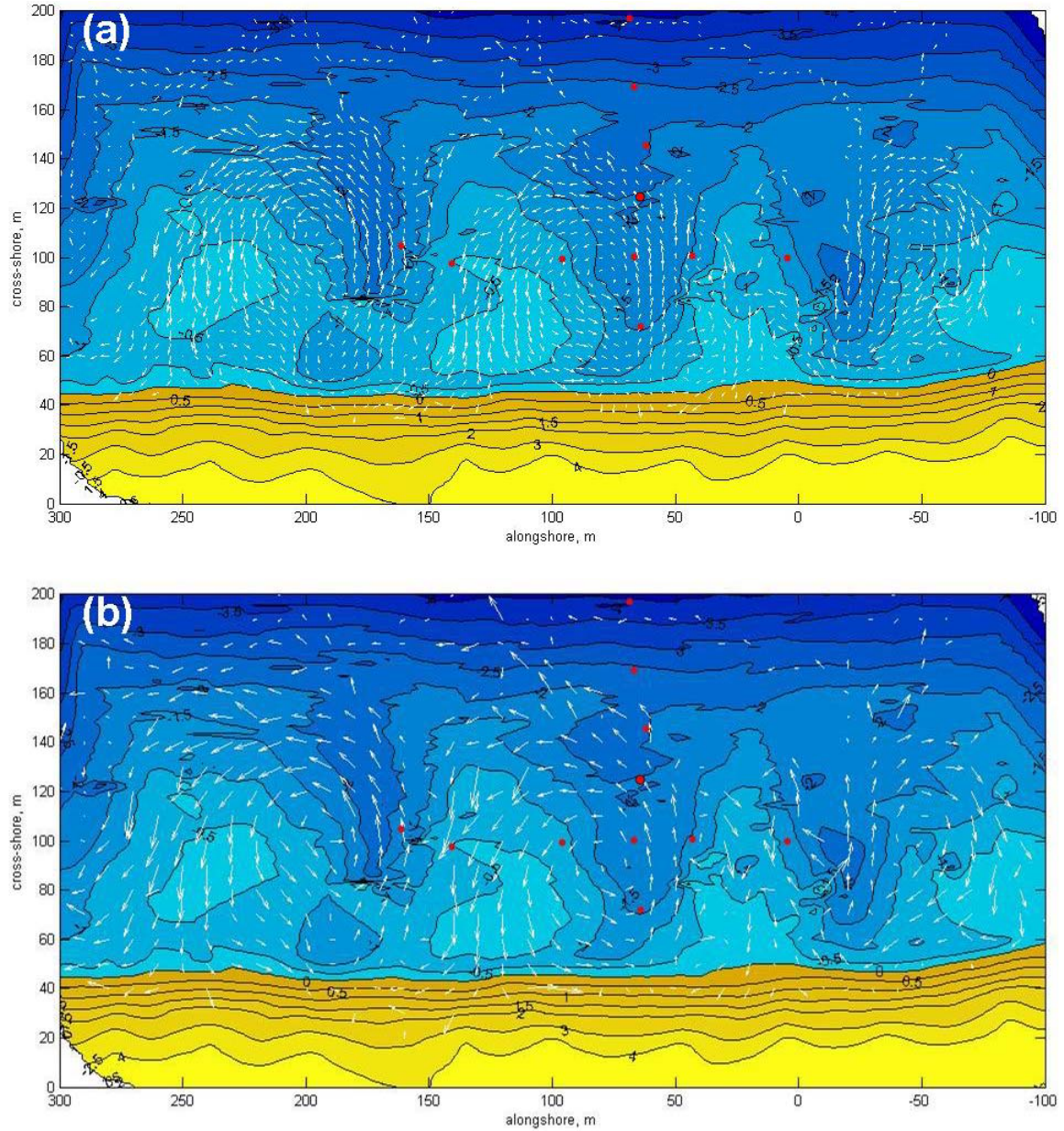


Figure 15. Bin-averaged velocity vectors plotted against bathymetry using: (a) $5m \times 5m$ grid spacing; and (b) $10m \times 10m$ grid spacing. The average shoreline for the deployment period is represented by the border between yellow contours (sand) and blue contours (water). Arrows are vectors of averaged velocities within each bin. Vectors shoreward of the shoreline are the result of tidal changes in the mean-water level during the deployment and possibly from imperfect removal of points during quality control. The smaller bin size provides finer resolution, but introduces more noise, while the larger bins provide smoother profiles at the expense of slightly lower resolution.

4. Bathymetric Adjustment

While underlying beach morphology at the field site changes little over time, tides still change the bathymetric mean sea level (*0m* contour) with time. To obtain bathymetry relevant to a particular deployment period, an adjustment is made to bathymetric surveys. Hourly mean sea levels for each PUV are computed relative to the same *0m* contour used in the bathymetric survey. These hourly averages are further averaged over a deployment period of interest. Bathymetry for the most relevant survey is adjusted by this second average to obtain bathymetry for a given deployment.

THIS PAGE INTENTIONALLY LEFT BLANK

IV. RESULTS

A. RIP CHARACTERISTICS

To determine rip current and rip channel characteristics, cross-shore velocity and bathymetric profiles for rip channels are averaged daily and for the entire experiment. Alongshore velocity and bathymetric profiles are also averaged for the entire experiment.

1. Rip Currents

Cross-shore velocities down the center of a rip channel (Figure 16) increase to a maximum of 50cm/s at about 50m from the shore. Beyond 50m , the velocities decay to about 20cm/s , with another small peak at about 100m , after which they decay again. The peak in velocities at 100m is likely a result of fewer observations and a bias towards higher velocities as drifters get caught in rip pulsations that eject them from the surf zone. Average rip current velocity is 30cm/s .

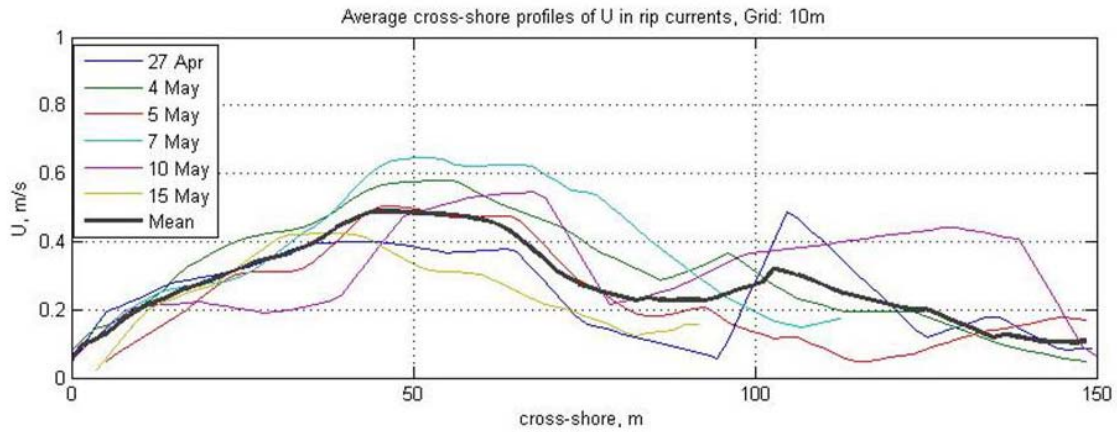


Figure 16. Cross-shore velocities in a rip channel. Cross-shore axis is normalized for the experiment to represent meters from the shoreline rather than meters from the local coordinate system alongshore axis.

2. Rip Channels

Cross-shore bathymetric profiles in the center of rip channels show increase in depth to about $1.5m$ at $50m$ from the shoreline. The slope for the first $50m$ is about 1:33. The profile from $50m$ to $100m$ is roughly flat, before becoming steep-sloped again after $100m$ (Figure 17).

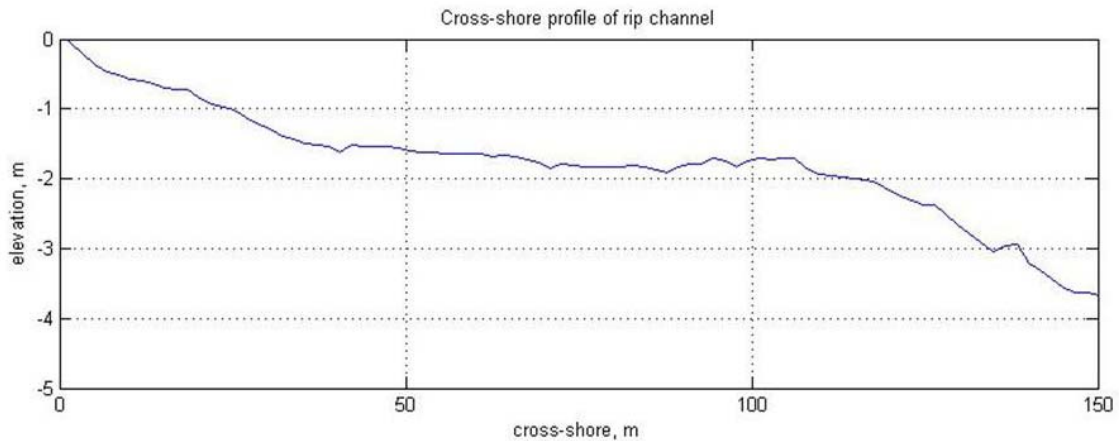


Figure 17. Cross-shore bathymetric profile in a rip channel. Cross-shore axis is normalized for the experiment to represent meters from the shoreline rather than meters from the local coordinate system alongshore axis.

Comparison of rip channel cross-shore velocity profiles to rip channel bathymetric profiles reveals a correlation between the maximum velocity and the change in slope at $50m$. The increase of slope at $100m$ also corresponds well to the edge of the surf-zone (e.g., breaker location) as found in time-lapsed imagery. With the apparent relationship between surf zone width and increasing slope leads, the end of the rip channel is defined as the end of the surf-zone. From this definition, the average channel length is $100m$, and the average maximum channel depth is $1.7m$.

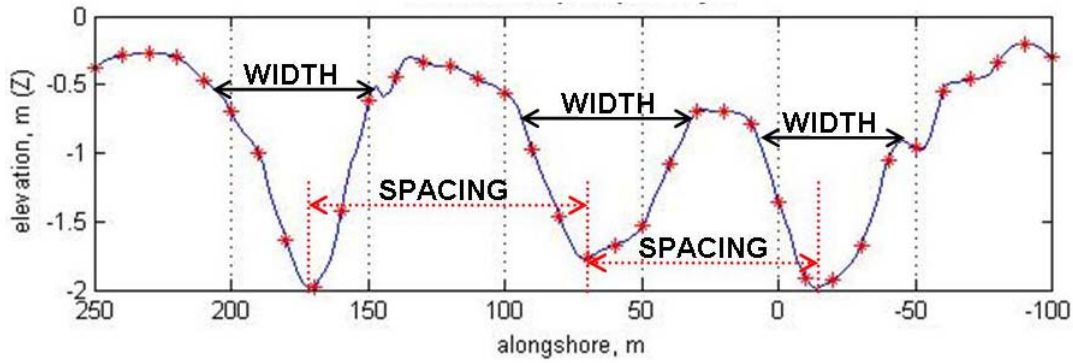


Figure 18. Alongshore bathymetric profile $\sim 50m$ from the shoreline, showing how rip-channel spacing and width were determined.

Alongshore bathymetric profiles are used to determine average width and spacing of rip channels (Figure 18). The profiles used are about $50m$ from the shoreline, where the maximum rip current velocities are found. Rip channel width is measured as the distance between greatest change in slope between the channel itself and the shoal on either side of the channel – the average width is $55m$. The channel spacing is the distance between depth maxima of adjacent rip channels – average channel spacing is about $90m$.

B. VOLUME BALANCE

Drifter data for 4 May shows gyres in surf-zone circulation centered at $95m$ and $105m$ offshore in local coordinates. Since $10m$ bins provide a smoother velocity profile than $5m$ bins, the larger bins were used for calculations of volumetric flow rate (Figure 19). The bin velocities were further smoothed by averaging over four bins (from $80m$ to $110m$) in the cross-shore direction.

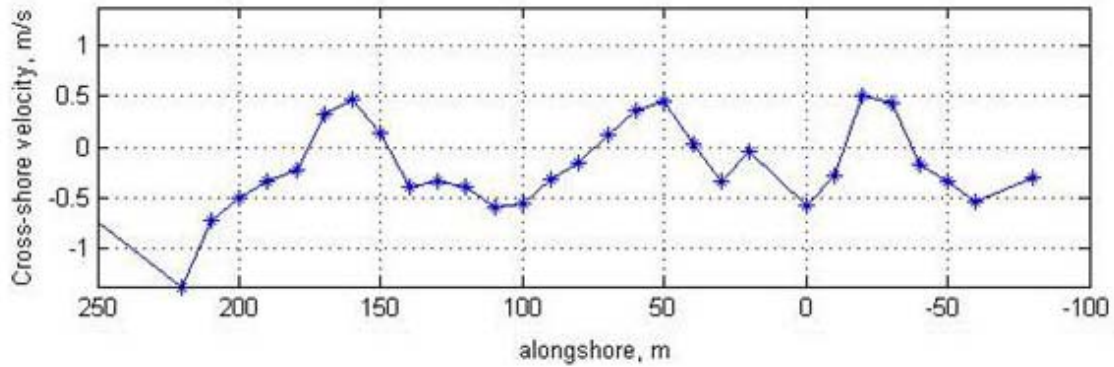


Figure 19. Alongshore profile of cross-shore velocities $\sim 50m$ from the shoreline. Positive velocities are off-shore, while negative velocities are onshore.

To verify continuity, a bathymetric profile is taken along a transect $\sim 50m$ from the shoreline. Discrete volumetric flow (V) is then calculated along the transect by:

$$V = uh \cdot \Delta y$$

where u is the bin average cross-shore component of velocity for the given point, h is depth of the water column at that point, and Δy is the bin width. This assumes no vertical shear in the water column. Summing the discrete volumetric flow rate over two gyres (from $30m$ to $220m$ alongshore) gives an offshore discharge of $\sim 58.62m^3/s$ and onshore discharge of $\sim 58.56m^3/s$. Net discharge is $\sim 0.0646m^3/s$, which is an error of less than 0.1% considering the gross discharge is $\sim 117m^3/s$ (Figure 20). Performing similar balances for profiles on 5 May, 7 May, and 10 May yields an overall average net-discharge imbalance of about 6.67% with a standard deviation of 4.79%.

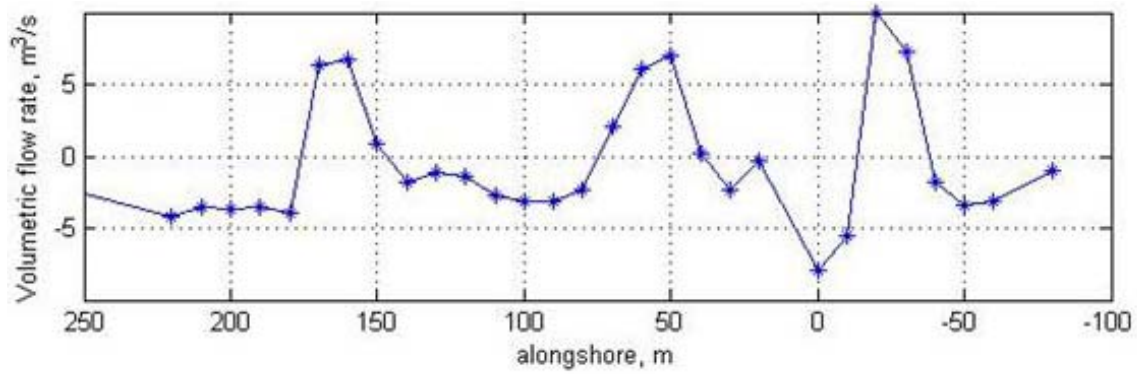


Figure 20. Volumetric flow rate profiles along transect located ~50m from the shoreline – positive is offshore flow.

The peaks in Figure 20 roughly correspond to rip-channel centers while valleys correspond to shoals. As expected from continuity, the flow rate over the shoals is characterized by a relatively flat valley along the width of the shoal, while flow in the rip channel is characterized by a narrower peak of greater magnitude.

C. EDDY CHARACTERISTICS

Drifter data for each day is sectioned into individual deployments. Each of those individual deployments are plotted and examined to find those with enough oscillatory motion to facilitate a general description of circulation cell characteristics for each day and for the site overall. The time-series of cross-shore drifter positions are demeaned, detrended, and auto-correlated for each deployment. At a lag of $\tau = 0s$ the auto-correlation function of the demeaned, detrended data is equal to the variance ($R_{xx}|_{\tau=0} = \sigma_x^2$), which permits calculation of the standard deviation. Since 95% of a dataset is contained within two standard deviations of its mean, the eddy radius is defined as $2\sigma_x$. Since diameter is twice the radius, eddy diameter is $4\sigma_x$. Period of rotation corresponds to the first lag ($\neq 0s$) where the auto-correlation function is a maximum. (Figure 21; Table 1)

Based on analysis of drifter data from days on which eddies were observed, the mean eddy diameter for the experiment is 88m and the mean period is 4.7min. On average, each drifter experienced at least eight revolutions in the surf zone before landing

on shore or heading outside the surf zone. The consistency of these data and their correspondence to surf zone characteristics (e.g., surf zone width) indicate that these eddies are real and persistent.

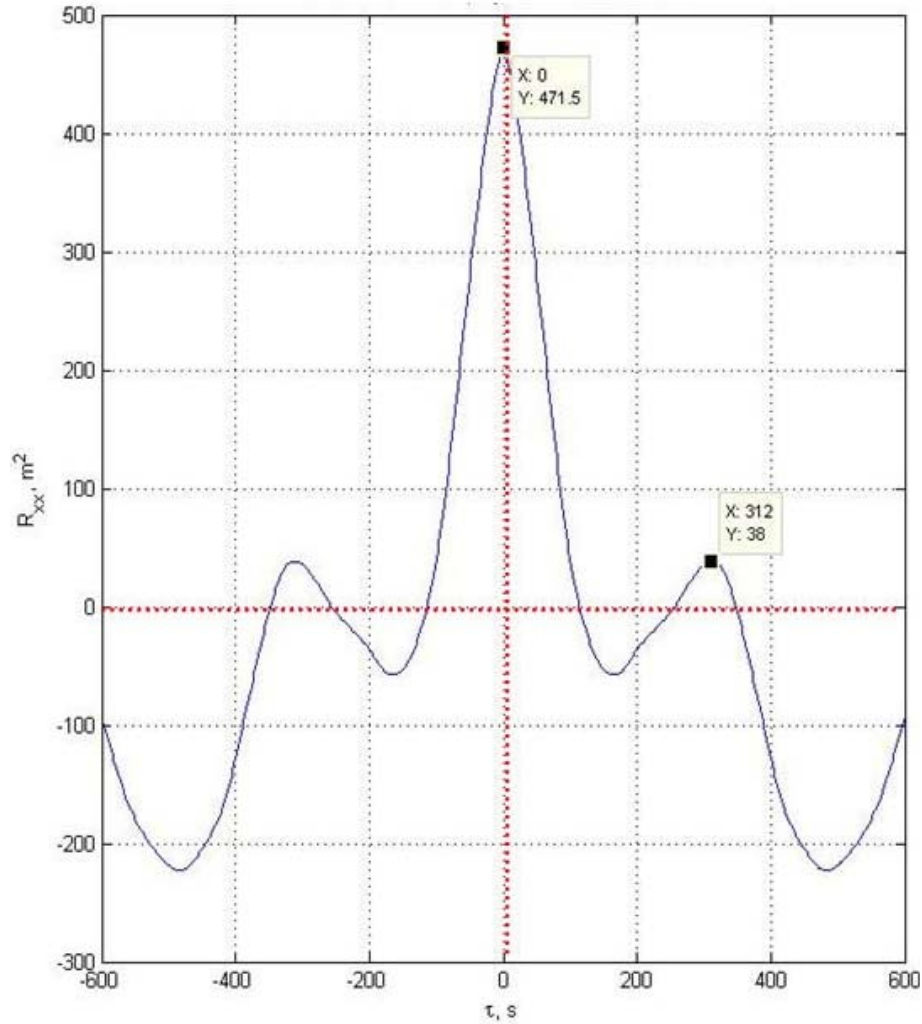


Figure 21. Sample autocorrelation plot of cross-shore positions. Lag (seconds) is the x-axis and auto-correlation value (m^2) is the y-axis. Since the auto-correlation is based on demeaned and detrended data, the peak at zero lag represents the square of the data variance. The value of lag at the next peak in auto-correlation corresponds to the period of oscillation for the data set.

	Average Diameter	Period
27 Apr 07	92.0 <i>m</i>	267 <i>s</i> (4.5 <i>min</i>)
4 May 07	86.0 <i>m</i>	255 <i>s</i> (4.3 <i>min</i>)
5 May 07	91.6 <i>m</i>	285 <i>s</i> (4.8 <i>min</i>)
7 May 07	82.8 <i>m</i>	319 <i>s</i> (5.3 <i>min</i>)
10 May 07	16.9 <i>m</i>	240 <i>s</i> (4.0 <i>min</i>)
15 May 07	12.9 <i>m</i>	307 <i>s</i> (5.1 <i>min</i>)
Overall Average	88.0 <i>m</i>	282 <i>s</i> (4.7 <i>min</i>)

Table 1. Eddy characteristics for the six deployment days with any observed eddies. The “overall” average excludes measurements from 10 May and 15 May – even though eddies were observed on those days, flow was primarily alongshore.

D. OBSERVATION DENSITY

An interesting feature of the eddies is their fairly persistent center positions. The highest number of observations occurs near the center of each circulation pattern on an observation density plot (Figure 22). This indicates that, during the deployment, drifters spend a significant amount of time near the eddy centers – observations are 2*s* apart and average velocities are lower at the eddy centers than the edges. This is an interesting phenomenon that could have an impact on pollution or biota transport (Talbot and Bate, 1987).

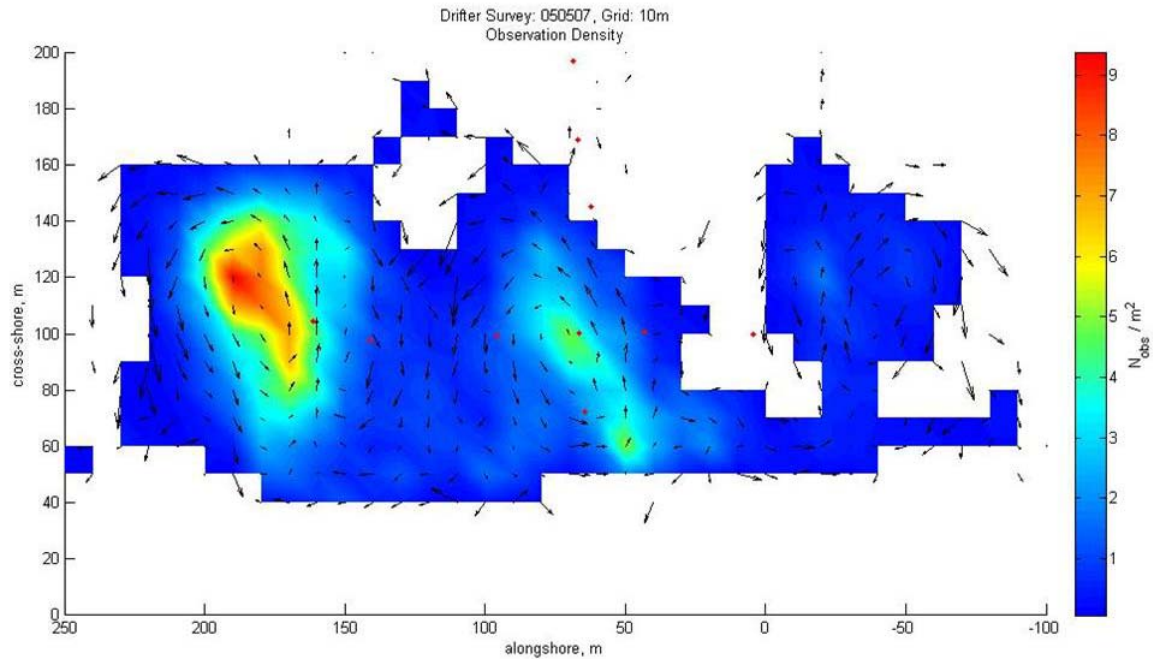


Figure 22. Observation density plot, showing higher concentration of drifter observations at the centers of surf zone eddies.

E. EULERIAN COMPARISON

To validate drifter observations they are compared with in situ instruments that are already widely accepted as correct. Hourly means of the PUV and ADCP recorded speeds are compared with corresponding hourly means of drifter speeds within 10m bins centered on each instrument in the array. Bins with fewer than 30 observations are filtered out since they are statistically insignificant. A scatter plot of the remaining speeds reveals a “shot-gun” pattern; however the linear regression is close to a one-to-one fit with an r^2 of 0.81 (Figure 23).

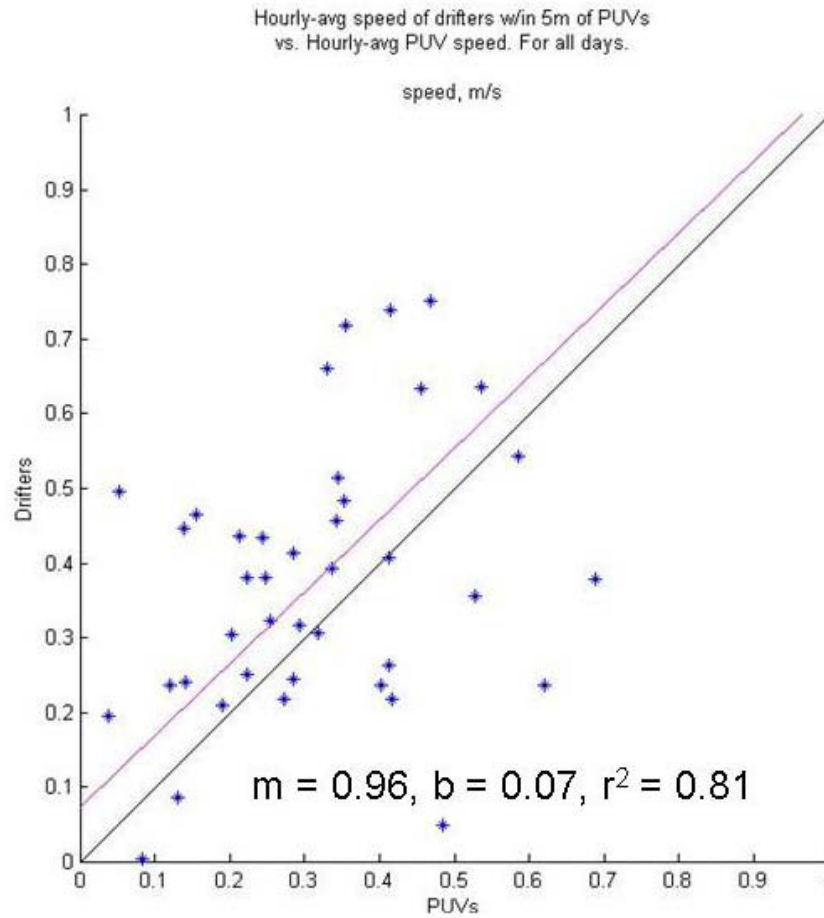


Figure 23. Results of a linear regression comparing average in situ instrument velocities with average drifter velocities near them. While there is scatter in the data correlation is relatively high (r-squared of 0.81,) with a best fit slope just less than one, and y-intercept only slightly larger than zero.

THIS PAGE INTENTIONALLY LEFT BLANK

V. CONCLUSIONS

A. SUMMARY

1. General Characteristics

Rip current circulation cells are found to be contained within the surf zone. The surf zone is the energetic region that extends from the shoreline to the offshore location where waves begin to break. The beach profile transitions from a low-tide terrace (slope $\sim 1:100$) to an offshore slope (about $1:20$) approximately $100m$ from the shoreline, which is the surf zone width. Rip channel length scales are characterized by an alongshore spacing of $O(90m)$, cross-shore channel length of $O(100m)$, and channel width of $O(55m)$. The morphodynamic relationship for this site is governed by wave breaking and bathymetry, generating patterns of onshore flow over shoals and offshore flow in narrow channels, rip currents.

Cross-shore velocities in the rip current increase from zero at the shoreline, to a maximum of $O(60cm/s)$ midway through the surf zone, and decay to the edge of the surf zone. An additional smaller peak in velocities was observed to occur at the edge of the surf zone, and is believed to be related to rip current pulsations. Average rip current velocities are $30 \pm 15 cm/s$ for seven deployments at various wave and tidal conditions.

Drifters deployed during RCEX demonstrate the presence of persistent surf zone eddies characterized by semi-closed loops related to the rip current circulation. These eddies complete a rotation in about $4.7min$, and are about $88m$ in diameter. Continuity of shoreward and seaward discharge calculations about $50m$ from shore (near the eddy centers) balance to less than 10% of the gross discharge.

2. Drifter Performance

With ground-breaking success, a low-cost drifter has demonstrated its ability to significantly improve our picture and understanding of the horizontal flow structure near shore and fill in gaps left by using only in situ instruments. Comparison of average

drifter speeds near in situ instruments shows relatively high correlation between the two measurements. The r-squared value of ~0.81 for a linear regression fit between the two sets of data demonstrates that drifter speeds compare well with speed obtained by in situ instruments that are already accepted as accurate.

3. Setting the Record Straight

The prevailing opinion is that the best way out of a rip current is to swim parallel to shore – this is not necessarily good advice. The presence of eddies on either side of a rip current suggest that a swimmer would at best have a 50% chance of swimming with the current by swimming parallel to the shore. A swimmer has a better chance of conserving energy and returning to land safely by floating with the current and letting it carry him back to shore with the onshore flow of the eddy. In doing so, the swimmer will still need to deal with oncoming waves, especially as he nears the edge of the surf zone, but he will expend less energy in the process.

B. OTHER WORK

1. Current Research

Since RCEX only took place six months ago, this thesis contains the preliminary results of a much larger picture of rip current circulation dynamics. Other research in progress based on the experiment includes: measurement of dispersion and diffusivity based on multi-particle statistics through the drifters; investigation of the effect of waves/tides on circulation cells and possible rip current pulsations; and examination of the poor correlation between individual velocity components of the Lagrangian and Eulerian measurements.

2. Future Research and Improvement

Other interesting research that could stem from this are: exploration of the role these circulation patterns play in sediment transport; or examination of the effect of these

nearshore circulation patterns on humans by making similar measurements using human “drifters.” It would also be useful to extend these results to modeling in order to better predict flow behavior near shore.

Future experiments similar to RCEX could be improved by finding some way to turn the logging devices on and off without having to open the water-proof boxes during deployment, thus reducing error introduced by humans. It might also prove useful to have a compass as an integral part of the in situ instruments to eliminate human error associated with determining their orientation.

3. Application

The results presented here have a direct application to the Navy. SEAL and mine-hunting operations both deal directly with the surf-zone. An understanding of the rip current circulation patterns in the surf zone will improve predictive modeling and aid in planning mine-hunting and SEAL delivery.

THIS PAGE INTENTIONALLY LEFT BLANK

LIST OF REFERENCES

- Bowen, A.J., Rip currents: 1. Theoretical investigations, *Journal of Geophysical Research*, 74(23), 5467-5478, 1969.
- Bowen, A.J., and D.L. Inman, Rip currents: 2. Laboratory and field observations, *Journal of Geophysical Research*, 74(23), 5479-5490, 1969.
- Brander, R.W., Field observations on the morphodynamic evolution of a low-energy rip current system, *Marine Geology*, 157, 199-217, 1999.
- Dalrymple, R.A., A mechanism for rip current generation on an open coast, *Journal of Geophysical Research*, 80(24), 3485-3487, 1975.
- Dalrymple, R.A., Rip currents and their causes, *Proc. 16th Int. Conf. Coastal Eng.*, 1414-1427, 1978.
- Dalrymple, R.A., and C.J. Lozano, Wave-current interaction models for rip currents, *Journal of Geophysical Research*, 83(C12), 6063-6071, 1978.
- Haller, M.C., R.A. Dalrymple, and I.A. Svendsen, Rip channels and nearshore circulation, *Coastal Dynamics*, 594-603, 1997.
- Haller, M.C., R.A. Dalrymple, and I.A. Svendsen, Experimental study of nearshore dynamics on a barred beach with rip channels, *Journal of Geophysical Research*, 107(C6), 3061, doi:10.1029/2001JC000955, 2002.
- Hammack, J., N. Scheffner, H. Segur, A note on generation and narrowness of periodic rip currents, *Journal of Geophysical Research*, 96(C3), 4909-4914, 1991.
- Hansen, J.B., and I.A. Svendsen, A theoretical and experimental study of undertow, *Proc. 19th Conf. Coastal Eng.*, 2246-2262, 1984.
- Johnson, D., and C. Pattiaratchi, Application, modeling and validation of surfzone drifters, *Coastal Engineering*, 51, 455-471, 2004.
- Johnson, D., and C. Pattiaratchi, Transient rip currents and nearshore circulation on a swell-dominated beach, *Journal of Geophysical Research*, 109, C02026, doi:10.1029/2003JC001798, 2004.
- Johnson, D., R. Stocker, R. Head, J. Imberger, and C. Pattiaratchi, A compact, low-cost GPS drifter for use in the oceanic nearshore zone, lakes, and estuaries, *Journal of Atmospheric and Oceanic Technology*, 20, 1880-1884, 2003.
- Kennedy, A.B., and D. Thomas, Drifter measurements in a laboratory rip current, *Journal of Geophysical Research*, 109, C08005, doi:10.1029/2003JC001927, 2004.

- MacMahan, J.H., A.J.H.M. Reniers, E.B. Thornton, and T.P. Stanton, Surf zone eddies coupled with rip current morphology, *Journal of Geophysical Research*, 109, C07004, doi:10.1029/2003JC002083, 2004.
- MacMahan, J.H., E.B. Thornton, and A.J.H.M. Reniers, Rip current review, 2005.
- MacMahan, J.H., E.B. Thornton, T.P. Stanton, and A.J.H.M. Reniers, RIPEX: Observations of a rip current system, *Marine Geology*, 218, 113-134, 2005.
- MacMahan, J.H., and J. Brown, An inexpensive hand-held global positioning system for oceanographic drifters, 2007.
- Ranasinghe, R., G. Symonds, K. Black, and R. Holman, Morphodynamics of intermediate beaches: a video imaging and numerical modeling study, *Coastal Engineering*, 51, 629-655, 2004.
- Schmidt, W.E., B.T. Woodward, K.S. Millikan, R.T. Guza, B. Raubenheimer, and S. Elgar, A GPS-tracked surf zone drifter, *Journal of Atmospheric and Oceanic Technology*, 20, 1069-1075, 2003.
- Schmidt, W.E., R.T. Guza, and D.N. Slinn, Surf zone currents over irregular bathymetry: Drifter observations and numerical simulations, *Journal of Geophysical Research*, 110, C12015, doi:10.1029/2004JC002421, 2005.
- Shepard, F.P., Undertow, rip tide or "rip current," *Science*, 34, 181-182, 1936.
- Shepard, F.P., K.O. Emery, and E.C. La Fond, Rip currents: A process of geological importance, *Journal of Geology*, 49(4), 337-369, 1941.
- Shepard, F.P., and D.L. Inman, Nearshore circulation, *Proc. 1st Int. Conf. Coastal Eng.*, 50-59, 1950.
- Short, A.D., and C.L. Hogan, Rip currents and beach hazards: Their impact on public safety and implications for coastal management. In Finkl, C.W. (ed.) *Coastal Hazards, Journal of Coastal Research*, Special Issue 12, 197-209, 1994.
- Sonu, C.J., Field observations of nearshore circulation and meandering currents, *Journal of Geophysical Research*, 77(18), 3232-3247, 1972.
- Talbot, M.M.B., and G.C. Bate, Rip current characteristics and their role in the exchange of water and surf diatoms between the surf zone and nearshore, *Estuarine, Coastal and Shelf Science*, 25, 707-720, 1987.

Wright, L.D., and A.D. Short, Morphodynamic variability of surf zones and beaches: A synthesis, *Marine Geology*, 56, 93-118, 1984.

United States Lifesaving Association, Rip Currents,
<http://www.usla.org/ripcurrents/default.asp>, valid 17 September 2007.

THIS PAGE INTENTIONALLY LEFT BLANK

INITIAL DISTRIBUTION LIST

1. Defense Technical Information Center
Ft. Belvoir, Virginia
2. Dudley Knox Library
Naval Postgraduate School
Monterey, California
3. Jamie H. MacMahan
Naval Postgraduate School
Monterey, California
4. Timothy P. Stanton
Naval Postgraduate School
Monterey, California
5. Edward B. Thornton
Naval Postgraduate School
Monterey, California
6. Mark Orzech
Naval Postgraduate School
Monterey, California
7. Ad Reniers
University of Miami
Miami, Florida
8. Edith Gallagher
Franklin and Marshall College
Lancaster, Pennsylvania
9. Rob Wyland
Naval Postgraduate School
Monterey, California
10. Jeff Brown
University of Delaware, Department of Coastal Engineering
Newark, Delaware
11. Jenna Brown
University of Delaware, Department of Coastal Engineering
Newark, Delaware